

Article

A Quantitative Method for Long-Term Water Erosion Impacts on Productivity with a Lack of Field Experiments: A Case Study in Huaihe Watershed, China

Degen Lin ^{1,2}, Hao Guo ^{1,2}, Fang Lian ^{1,2}, Yuan Gao ^{1,2}, Yaojie Yue ^{1,2,3} and Jing'ai Wang ^{1,2,3,*}

¹ School of Geography, Beijing Normal University, Beijing 100875, China; ldg@mail.bnu.edu.cn (D.L.); ghbnu@mail.bnu.edu.cn (H.G.); lianfang2023@mail.bnu.edu.cn (F.L.); gcaesar@163.com (Y.G.); yjyue@bnu.edu.cn (Y.Y.)

² Key Laboratory of Regional Geography, Beijing Normal University, Beijing 100875, China

³ State Key Laboratory of Earth Surface Processes and Resource Ecology, Beijing Normal University, Beijing 100875, China

* Correspondence: jwang@bnu.edu.cn; Tel.: +86-10-5880-7454 (ext. 1632)

Academic Editor: Luis Loures

Received: 13 June 2016; Accepted: 11 July 2016; Published: 19 July 2016

Abstract: Water erosion causes reduced farmland productivity, and with a longer period of cultivation, agricultural productivity becomes increasingly vulnerable. The vulnerability of farmland productivity needs assessment due to long-term water erosion. The key to quantitative assessment is to propose a quantitative method with water loss scenarios to calculate productivity losses due to long-term water erosion. This study uses the agricultural policy environmental extender (APEX) model and the global hydrological watershed unit and selects the Huaihe River watershed as a case study to describe the methodology. An erosion-variable control method considering soil and water conservation measure scenarios was used to study the relationship between long-term erosion and productivity losses and to fit with 3D surface (to come up with three elements, which are time, the cumulative amount of water erosion and productivity losses) to measure long-term water erosion. Results showed that: (1) the 3D surfaces fit significantly well; fitting by the 3D surface can more accurately reflect the impact of long-term water erosion on productivity than fitting by the 2D curve (to come up with two elements, which are water erosion and productivity losses); (2) the cumulative loss surface can reflect differences in productivity loss caused by long-term water erosion.

Keywords: long-term water erosion; productivity loss; 3D surface

1. Introduction

The soil controls the hydrological, erosional, biological, ecological and geochemical cycles and is also important for humankind as the source of goods, resources and services [1–4]. Approximately 80% of the world's agricultural land suffers moderate to severe land degradation due to long-term soil erosion [5], such as Africa [6], Europe [7–9], South America [10] and Asia [11]. Cropped land is particularly vulnerable to erosion due to the exposure of bare soil for lengthy periods and the disturbance of the soil structure during farming operations, such as tillage [12]. Long-term water erosion results in the loss of organic matter and, as a consequence, the loss of production and the elimination of fertile land [13–15]. As a result of long-term water erosion, over the last 40 years, about 30% of the world's cropland has become unproductive, and much of it has been abandoned [5,16]. Each year, an estimated 10 million ha of cropland worldwide are abandoned due to the loss of productivity caused by water erosion [17–19]. This in turn threatens food security and poverty, as well [20,21], and

affects the sustainable development of agriculture. A quantitative assessment of farmland yield loss caused by long-term water erosion is thus important.

The methods used to assess farmland yield loss are mainly long-term field experiments and model simulations under soil loss scenarios. In long-term field experiments, the relationship between water erosion (amount of water erosion or erosion depth) and crop yield is evaluated with a dimensional curve [22]. Gao et al. [23] conducted a long-term field experiment and established the relationship between erosion depth and the reduction of yield and biomass of the past 10 years by a dimensional curve. Larney et al. [24] set erosion depths (0, 5, 10, 15 and 20 cm) of surface soil, which were removed to represent different erosion severity for the past 16 years, and used multiple dimensional curves to find the relationship between water erosion and crop yield. The long-term field experiment method can more accurately simulate the dynamic change and the reduction of yield due to water erosion at present. However, it needs long-term measured data in the field, and there are difficulties to characterize the relationship of yield loss with long-term water erosion by limited field experiments [25].

The model simulation method was used to simulate soil erosion and productivity under soil loss scenarios based on the natural, process-based simulation model [26]. Ye and Van Ranst [26] used land degradation scenarios (the no degradation scenario, the current scenario and the double degradation scenario) to quantify the long-term water erosion impact on food crops based on the web-based land evaluation system (WLES) model. However, the yield loss they simulate considered little the cumulative amount of water erosion. Other studies [22,23] have found that with a longer planting time, there would be a cumulative increase in the amount of water erosion and an accelerated reduction in crop yield. Therefore, the combination of the WLES model and land degradation scenarios is not suitable for expressing the relationship between the cumulative amount of water erosion and the loss in productivity.

In order to assess the effect of long-term water erosion on a large or global scale, an effective method with the 3D (three-dimensional) surface [27] considering accumulated soil loss scenarios is needed. The method comes up with three elements, which are time, the cumulative amount of water erosion and losses in agricultural productivity. The 3D surface is able to quantify the relationship by three elements, while the 2D curve can only express two elements, which are soil erosion and productivity losses [24,28].

This paper proposes a quantitative method with the 3D surface to calculate productivity loss due to long-term water erosion at a large scale with a lack of field experiments. This paper selected the agricultural policy environmental extender (APEX) model with localization parameters to estimate soil erosion and its effect on crop. After that, an erosion variable-controlled method was used to consider the effect of the cumulative amount of water erosion and the developed 3D surface to (come up with three elements, which are time, the cumulative amount of water erosion and productivity losses) based on the logistic curve model [28] to study the relationship between long-term erosion and productivity loss. The 3D surface is important for understanding the effects of long-term erosion on productivity.

2. Materials and Methods

2.1. Study Area

This paper chose the middle and upper reaches of the Huaihe River watershed as the study area, as shown in Figure 1. The Huaihe River watershed is one of the seven major river watersheds in China. It flows from the west to the east, bordering the Huanghe River (Yellow River) in the north and the Yangtze River in the south. Starting in the Tongbai Mountains in Henan province, its waterway is about 1000 km long, and its catchment area is about 1.9×10^5 km² [29]. The area of its cropland is 120,542 km², and the cropland is characterized by extreme slopes covering 10,413 km² of the overall cropland area. Water erosion rates as high as 35 Mg·ha⁻¹·year⁻¹ occur across nearly 22% of the watershed area. Inappropriate land use practices, such as extensive cultivation, cultivating on steep slopes (over 27%) and deforestation, in combination with the lack of conservation practices and mismanaged construction

projects, aggravate water-induced erosion [30]. Average annual precipitation is 728 mm; the yearly average maximum daily temperature is 20.6 °C; and the yearly average minimum daily temperature is 10.0 °C. The main crops are maize and rice. Based on HydroSHEDS (WWF, Washington, DC, USA), the study area can be divided into 21 small watershed units and 68 subarea units.

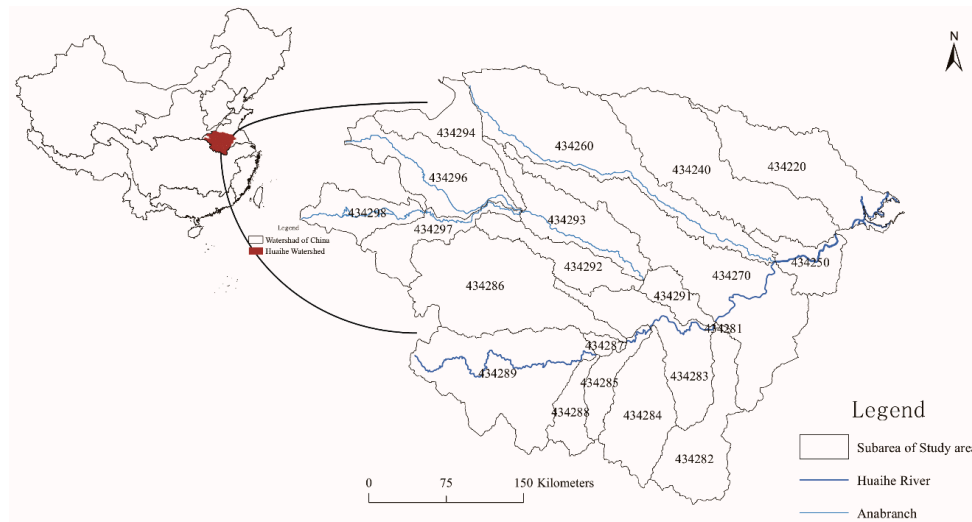


Figure 1. Study area (the basin ID was adopted from HydroSHEDS).

The APEX model was developed to extend the Environmental Policy Integrated Climate (EPIC) model [31] capabilities to whole farms and small watersheds, based on watershed and subarea units [32]. According to the HydroSHEDS basin [33], the world can be divided into a subarea global scale to fit the APEX model precision requirement. The most important data for each subarea, such as weather and environment, were used as input data to simulate the characteristics of each watershed.

2.2. Basic Idea and Research Framework

- Numerical simulation of the natural geography process:

Natural, process-based simulation models can help to interpret complex natural geography process, environmental evolution and policy [34,35]. The agricultural policy environmental extender (APEX) model was developed to estimate soil productivity as affected by erosion, and it simulates approximately eighty crops with a crop growth model using unique parameter values for each crop [34,36]. The APEX model was constructed to evaluate various land management strategies considering sustainability, erosion (wind, sheet and channel), economics, water supply and quality, soil quality, plant competition, weather and pests [34]. Based on localization parameters and localization data, the APEX model can effectively simulate the natural environment process of the study area. Therefore, this paper selected the APEX model with localization parameters to estimate soil erosion and its effect on crops.

- Relationship between erosion and productivity:

Currently, field experiments find that there is a cumulative effect on productivity with long-term water erosion [22,23]. However, the models with soil loss scenarios consider little of the cumulative amount of water erosion. Therefore, this paper considered all water erosion scenarios from the most severe erosion scenario to the moderate to no erosion scenarios and used the yield under the no erosion scenario as the optimal yield, as well as the other yield under erosion scenarios as the erosion yield. The residual between the erosion yield and optimal yield is the yield loss by erosion. In each year, the yield loss by erosion was affected by the cumulative soil erosion. This study is concerned with the

productivity losses in particular years compared to the productivity in a scenario of no water erosion. Therefore, the length of time that the farmland had been planted was not considered.

- Logistic fitness model:

The logistic curve model could quantify the relationship of hazard and loss [28]. However, curves will lose the information when there are three elements, such as time, the cumulative amount of soil erosion and losses in agricultural productivity. The 3D surface was able to quantify the relationship by three elements [37], while the 2D logistic curve could only express two [24,28]. Therefore, this paper selected the 3D surface to quantify the long-term water erosion impact on food crops.

The study consists of three basic steps: (1) build the APEX model with the localization parameters and the localization data of the study area; (2) based on the erosion variable-controlled method, the long-term relationship between erosion and loss of productivity is constructed; (3) the cumulative years, the cumulative amount of water erosion and the loss of productivity are used to build the 3D surfaces expressed as water erosion intensity-cumulative years-yield loss. The research framework is described in Figure 2.

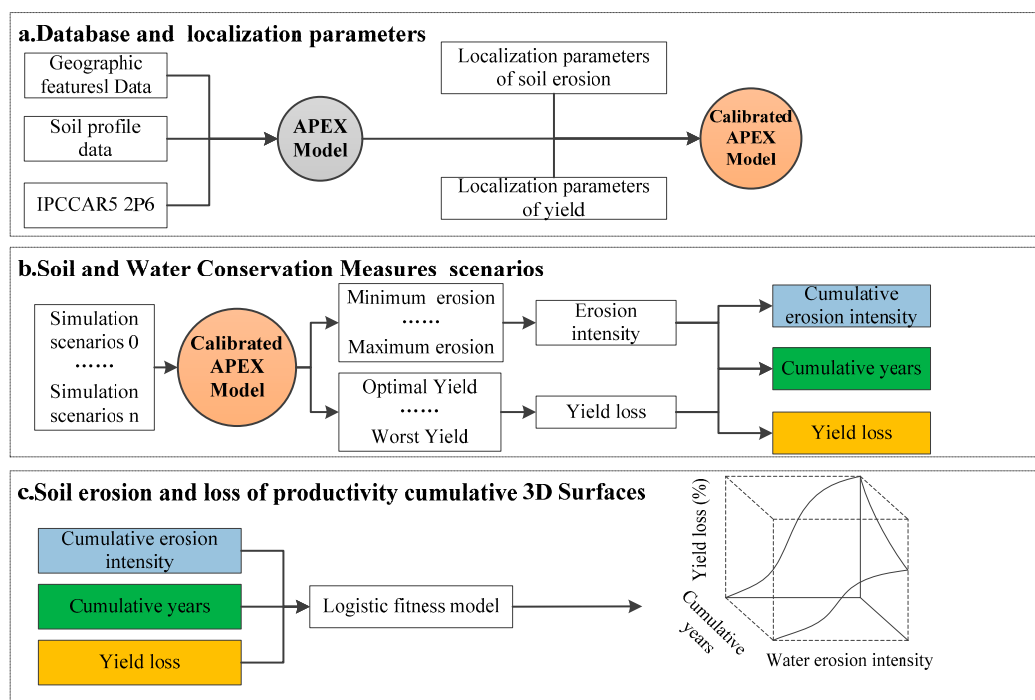


Figure 2. Research framework: (a) build the agricultural policy environmental extender (APEX) model with localization parameters and localization data of the study area in order to simulate long-term water erosion and productivity; (b) use the soil and water conservation measures' scenarios to get a group of samples of long-term water erosion intensity and yield and build the relationship between cumulative years, cumulative soil erosion and the yield loss, which is the residual between the erosion yield and optimal yield; (c) use the 3D surface based on the logistic model to quantify the loss of productivity affected by long-term water erosion.

We selected the middle and upper reaches of the Huaihe River watershed as a case and used the agricultural policy environmental extender (APEX) model [38], which is an emerging tool for landscape and watershed environmental analyses, as a tool to simulate erosion and productivity, and we used the IPCCAR5 scenario 2P6 data [39,40] as the long-term future climate data in the APEX model. Then, we built accumulated soil loss scenarios, with different soil and water conservation measure factors to represent accumulated erosion severity, and we used 3D surfaces to express the

relationship between the cumulative amount of water erosion, the loss of productivity and cumulative years; thus, we quantitatively assessed the loss of productivity due to long-term water erosion.

2.3. Data

Table 1 shows the contents of the database used for the global-scale water erosion evaluation.

Table 1. Datasets for global-scale water erosion evaluation.

Data Name	Data Content	Spatial Resolution	Temporal Resolution	Data Sources and url
DEM	Global elevation	0.00833° × 0.00833°	1997	USGS [41], ftp://edcftp.cr.usgs.gov/data/gtopo30/global/
Slope	Global slope	0.0833° × 0.0833°	1997	GAEZ [42], http://www.gaez.iiasa.ac.at/
Soil Properties	Global soil distribution raster image and physical and chemical characteristics, such as: pH, soil depth and other information	0.0833° × 0.0833°	1995	ISRIC, http://www.isric.org/data/isric-wise-derived-soil-properties-5-5-arc-minutes-global-grid-version-12 [43]
Meteorological	Global precipitation, temperature, solar radiation and other information	0.5° × 0.5°	1971–2099	Inter-Sectoral Impact Model Intercomparison Project RCP2.6 [44], http://pcmdi9.llnl.gov/
Planting Area	Global cultivation crop region	0.0833° × 0.0833°	1992	Sustainability and the Global Environment, University of Wisconsin-Madison [45], http://nelson.wisc.edu/sage/data-and-models/1992-croplands/index.php
Growth Period	Planting time and growth period length	0.0833° × 0.0833°	2000–2015	Nelson Institute for Environmental Studies at the University of Wisconsin-Madison [46], http://nelson.wisc.edu/sage/data-and-models/crop-calendar-dataset/index.php ; China's crop growth and soil moisture late value farmland collection data [47], http://data.cma.cn/data/detail/dataCode/AGME_AB2_CHN_TEN.html
Irrigation	Global annual irrigation water of agriculture(mm)	0.5° × 0.5°	1995	Institute of Industrial Science, University of Tokyo [48], http://hydro.iis.u-tokyo.ac.jp/GW/result/global/annual/withdrawal/index.html
Fertilizer	Global annual fertilizer application for maize	0.0833° × 0.0833°	2012	Earth stat [49], http://www.earthstat.org/data-download/
River basin unit	Global hydrological data	Vector unit	2010	HydroSHEDS [33], http://hydrosheds.cr.usgs.gov/index.php

According to the Paris Agreement [50], the expected key result was an agreement to set a goal of limiting global warming to less than 2 degrees Celsius (°C), and the IPCCAR5 scenario 2P6 [38,39] was similar to the Paris Agreement. Therefore, the IPCCAR5 scenario 2P6 was adopted as the meteorological data, and productivity losses for 2000–2099 were simulated based on the year 2000.

Based on the APEX model requirements, the most important environmental data (such as slope, elevation) and field management data were used to simulate each watershed and subarea as Table 2. The basin number adopted a HydroSHEDS number. The soil number was adopted from the ID provided by FAO and ISRIC. The field management data were adopted from the average agro-meteorological station data for the study area; the sowing time is 8 June; the harvest time is 15 September; and the farming system is sole cropping. Meteorological data were adopted from the IPCCAR5 scenario 2P6 in the study area. The daily maximum temperature, daily minimum temperature, daily relative humidity, daily solar radiation and daily wind speed from 2000–2099 were input into the APEX model.

The study area includes four dominant soil types [43], Mollic Gleysols (4339), Eutric Gleysols (4329, 4326), Calcaric Gleysols (4319), lithosols with Chromic Cambisols (3085) [43]. The soil property stratification data are shown in Table 3.

Table 2. Major natural geographic features and attributes of the field management of maize.

Basin Number	Slope (°)	Elevation (m)	Basin Area (ha)	Farming Area (ha)	Soil ID *	Irrigation (mm)
434220	2	30	936,950	5380	4339	15
434240	2	34	1,314,620	5296	4339	68
434250	5	25	312,450	3264	4329	614
434260	2	43	1,526,660	6302	4319	68
434270	2	28	1,662,910	8386	4326	83
434283	2	23	712,520	6811	4326	97
434282	30	31	672,040	10	3085	0
434284	16	56	678,050	6880	3085	8
434285	5	59	240,920	550	4326	1220
434291	2	27	200,540	4115	4339	310
434293	2	52	633,070	6949	4319	51
434292	2	46	406,800	4819	4319	189
434286	2	43	1,313,270	8133	4319	11
434287	2	27	56,680	4924	4326	86
434288	5	50	233,960	695	4326	86
434289	2	45	1,309,830	4966	4326	48
434294	2	88	607,860	5692	4319	113
434297	2	71	388,330	2185	4319	33
434296	2	53	694,240	1450	4319	2
434298	8	52	357,500	941	3085	0
434281	5	23	6830	10	4326	0

* Note: The soil ID was adopted from FAO and ISRIC.

Table 3. Soil properties used in the simulation for the study site.

Property Soil ID	Soil Layer	Depth (m)	Bulk Density (Mg. m ⁻³)	Soil Water Content at Field Capacity (mm ⁻¹)	Sand (%)	Silt (%)	Soil pH	Organic Carbon (%)	Cation Exchange Capacity (cmol/kg)	Coarse Fragment (%)	Electrical Conductivity (mmho/cm)
4339	1	0.2	1.35	0.17	27	36	6.36	24.16	28.4	4	0
	2	0.4	1.34	0.16	29	33	6.61	13.97	24.5	6	0.33
	3	0.6	1.38	0.17	29	33	6.73	7.06	23.8	9	0.41
	4	0.8	1.38	0.19	31	32	6.95	4.95	21.94	10	0.51
	5	1	1.39	0.19	34	31	7.13	3.98	19.97	9	0.38
4329	1	0.2	1.24	0.21	37	34	6.02	13.12	16.09	8	0
	2	0.4	1.37	0.16	36	31	6.15	5.71	15.14	11	0
	3	0.6	1.4	0.15	36	30	6.28	4.01	14.47	14	0
	4	0.8	1.43	0.15	37	29	6.38	3.02	14.56	16	0
	5	1	1.46	0.16	36	29	6.48	2.79	15.18	18	0
4326	1	0.2	1.24	0.21	37	34	6.02	13.12	16.09	8	0
	2	0.4	1.37	0.16	36	31	6.15	5.71	15.14	11	0
	3	0.6	1.4	0.15	36	30	6.28	4.01	14.47	14	0
	4	0.8	1.43	0.15	37	29	6.38	3.02	14.56	16	0
	5	1	1.46	0.16	36	29	6.48	2.79	15.18	18	0
4319	1	0.2	1.27	0.19	35	27	7.29	9.23	21.11	7	1.07
	2	0.4	1.55	0.16	33	29	7.66	4.97	16.72	9	1.84
	3	0.6	1.57	0.16	39	26	8.01	3.16	14.58	10	1.7
	4	0.8	1.61	0.16	38	25	8.06	2.16	15.75	12	2.8
	5	1	1.43	0.16	41	24	8.31	1.91	13.51	13	2.73
3085	1	0.1	1.34	0.12	47	30	7.01	20.88	16.28	24	1.74

2.4. Methodology

2.4.1. APEX Water Erosion and Localization Parameters

The APEX model can be subdivided into nine separate components defined as weather, hydrology, soil erosion, nutrients, soil temperature, plant growth, tillage, plant environment control and economics [32,51]. The APEX component for water-induced erosion simulates erosion caused by rainfall and runoff and by irrigation (sprinkler and furrow). To simulate rainfall/runoff erosion, APEX contains seven equations: the USLE [52], the Onstad–Foster modification of the USLE [53], RUSLE [54], the MUSLE [32], two recently-developed variations of MUSLE and an MUSLE structure that accepts input coefficients. The USLE depends strictly on rainfall as an indicator of erosive energy. However, it provides only annual estimates. The MUSLE and its variations use only runoff variables to simulate erosion and sediment yield. Runoff variables increase the prediction accuracy, and the MUSLE is calculated by (1) and (2).

$$Y = X \times EK \times CVF \times PE \times SL \times ROKF \quad (1)$$

$$X = 1.586 \times (Q \times q_p)^{0.56} \times WSA^{0.12} \quad (2)$$

where Y is the sediment yield in $t \cdot ha^{-1}$, EK is the soil erodibility factor, CVF is the crop management factor, PE is the erosion control practice factor, SL is the slope length and steepness factor, $ROKF$ is the coarse fragment factor, Q is the runoff volume in mm, q_p is the peak runoff rate in $mm \cdot h^{-1}$ and WSA is the watershed area in ha.

The parameters and sensitivity parameters were used for the study area. The parameters and the value of water erosion are the curve number for moisture Condition 2 (CN2), which is 65, the curve number index coefficient (CNIC), which is 1.5, conservation practice factor (PEC), which is 0.72, and the peak runoff rate rainfall energy adjustment factor (APM), which is 0.1 [30].

2.4.2. Soil and Water Conservation Measure Scenarios

We used an erosion control variable method to study the relationship between long-term erosion and productivity loss. Only the erosion was changed, and the remaining factors (such as weather, field management practices, fertilizer) were controlled and unchanged. The conservation measure factor was a number between 0 and 1. We set 12 conservation measures factors (0.01, 0.05, 0.1, 0.2, 0.3, 0.4, 0.5, 0.6, 0.7, 0.8, 0.9 and 1) as soil and water conservation measure scenarios to represent different soil and water conservation measures. The best soil and water conservation measure scenario represents the minimum soil erosion where the soil and water conservation measures factor is 0.01; the worst conditions and water conservation measures represent the maximum amount of potential soil erosion, where the soil and water conservation measures factor is 1.

2.4.3. Soil Erosion and Loss of Productivity

Based on the soil and water conservation scenarios, we used cumulative years, erosion intensity and loss of productivity to construct the surfaces.

- Productivity simulated by the APEX model:

A single model is used in APEX for simulating all of the crops considered (about 100). Each crop has unique values for the model parameters. APEX is capable of simulating growth for both annual and perennial crops. Annual crops grow from planting date to harvest date or until the accumulated heat units equal the potential heat units for the crop [55].

Soil erosion has affected the soil supply of nitrogen (N), phosphorus (P), potassium (K) and the depth of the soil layer [34,55,56]. Crop yield may be reduced through nutrient stress and temperature stress because of soil erosion [57,58].

- Loss of yield index calculation:

The yield loss index is defined here as the percentage of yield loss compared to the yield under the best conservation measure scenarios, and it is calculated using Equation (3).

$$Lr_i = \frac{(\max(y) - y_i)}{\max(y)} \quad (3)$$

where Lr_i is the yield loss index for crops due to soil loss under i conservation measure scenario, y_i is the yield under the i conservation measure scenario and $\max(y)$ is the yield under the best conservation measure scenario.

- Water erosion intensity calculation:

Water erosion is the cumulative soil erosion over cultivation years, and the water erosion intensity is the proportion of water erosion under the worst soil conservation measure scenario. It was calculated using Equation (4).

$$WE_i = \frac{\sum_{j=1}^n Se_i}{\sum_{j=1}^n Se_{\max}} \quad (4)$$

where Se_i is water erosion under i conservation measure scenario, $\sum_{j=1}^n Se_i$ is the water erosion after cumulative j year, $\sum_{j=1}^n Se_{\max}$ is the water erosion under the worst conservation measure scenario and WE_i is the water erosion intensity under the i conservation measure scenario.

- Cumulative loss 3D surface fitting:

From the basic idea section, we know that the 3D surface with the logistic model is better than the 2D logistic curve [28]. This paper established a cumulative loss 3D surface model by adding the cumulative years as the time dimension variable, calculated using Equation (5).

$$LR = \frac{(a/(1+b \times \exp(c \times WE_i)) - a/(1+b))}{(a/(1+b \times \exp(c)) - a/(1+b))} \times (d \times (i-e)^2 + f) \quad (5)$$

where a, b, c, d, e, f are the parameters of the surface model and LR is the loss yield index of crop due to soil loss under all kinds of conservation measures. i is the simulation of the cultivation i year, and WE_i is the accumulated soil loss after cultivation i year. As can be seen, in any year, the cultivation relationship is in the logistic curve shape.

2.4.4. Statistical Analysis

To confirm the significance of the results obtained by the cumulative loss 3D surface and the loss curve, we performed a paired t -test for all small watershed units [59–62]. The test statistic for the paired samples t -test, denoted t , follows the same formula as the one-sample t -test, calculated using Equations (6) and (7).

$$t = \frac{\bar{x}_{diff} - 0}{s_{\bar{x}}} \quad (6)$$

where:

$$s_{\bar{x}} = \frac{s_{diff}}{\sqrt{n}} \quad (7)$$

where \bar{x}_{diff} is the sample mean of the differences; n is the sample size (i.e., the number of all small watershed units); s_{diff} is the sample standard deviation of the differences; $s_{\bar{x}}$ is the estimated standard error of the mean (s/\sqrt{n}).

The calculated t -value is then compared to the critical t value with $df = n - 1$ from the t distribution table for a chosen confidence level. If the calculated t value is greater than the critical t value, then we conclude that the means are significantly different [62].

3. Results

3.1. Productivity Simulation and Verification

Summer maize was selected to evaluate its productivity in different water erosion scenarios and to provide information on the status of regional productivity. The simulated summer maize yield of Watershed 434298 (Lushan) and the observed yield of the Huaihe River Agricultural Meteorological Station were compared to calibrate the simulated yield as in Figure 3.

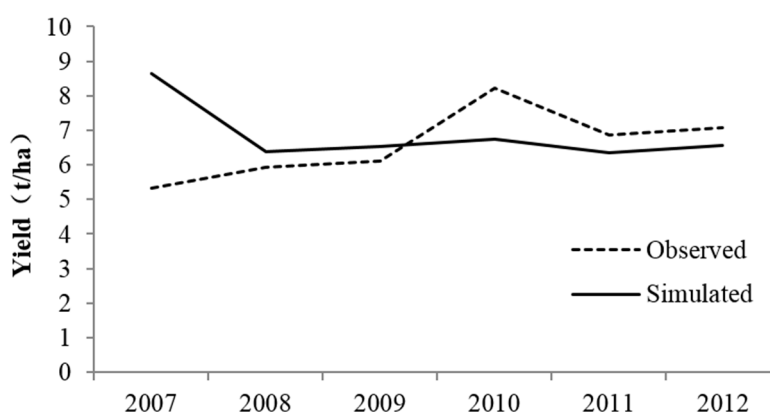


Figure 3. Simulated and observed yields in Huaihe River Watershed 434298 (Lushan).

Figure 3 shows the region’s productivity. In this region, the measured and simulated average yields were 6.58 t/ha and 6.87 t/ha, respectively, in 2007–2012. In 2007–2012 and 2008–2012, the RMSE was 1.53 and 0.78, respectively. Because the IPCCAR5 meteorological data had observed values for 1971–2004 and simulated values for 2005–2099, the simulated results contain an error, but the results still reflect the productivity level in the region.

3.2. Comparison of Cumulative Loss 3D Surfaces and 2D Curves

The key to comparing the 2D curve with the cumulative loss 3D surface is whether yield loss is affected by the cultivation year during long-term water erosion. For all watersheds, paired t -tests were used for testing the R-square of the 3D surface and 2D curve (Tables 4 and 5).

Table 4. Paired samples statistics of the surface and curve.

	Mean	N	Standard Deviation	Standard Error Mean
R-square of 3D Surfaces	0.772	21	0.078	0.017
R-square of 2D Curves	0.284	21	0.145	0.032

Table 5. Paired samples Student test.

	Paired Differences					t	df	Significance (2-Tailed)
	Mean	Std. Deviation	Std. Error Mean	95% Confidence Interval of the Difference				
				Lower	Upper			
R-square of Surface and R-square of Curve	0.488	0.162	0.035	0.414	0.562	13.813	20	0.000

From Tables 4 and 5, the mean R-square of the curve method is significantly lower than that of the surface method (paired samples t -test, $t = 13.813$, $df = 20$, 2-tail Significance (p) < 0.05) (Table 5). Thus, the mean R-square of the curve method and that of the surface method are significant. Therefore, fitting by the surface has a much higher R-square than fitting by the curve for all watersheds. The loss curve is fragmented, and the loss surface is continuous. The loss curve can be understood as a certain point in time on the surface. The loss surface has a more accurate meaning and expression. The surface fitting can thus more accurately reflect the impact of long-term water erosion on productivity.

3.3. Cumulative Loss 3D Surface from Long-Term Accumulated Water Erosion

We used the accumulated loss data of all of the hydrological response units in the Huaihe River watershed to construct a representation of the cumulative loss surface. Figure 4a shows a long-term loss rate of less than 100%, and Figure 4b shows a long-term loss rate of up to 100%.

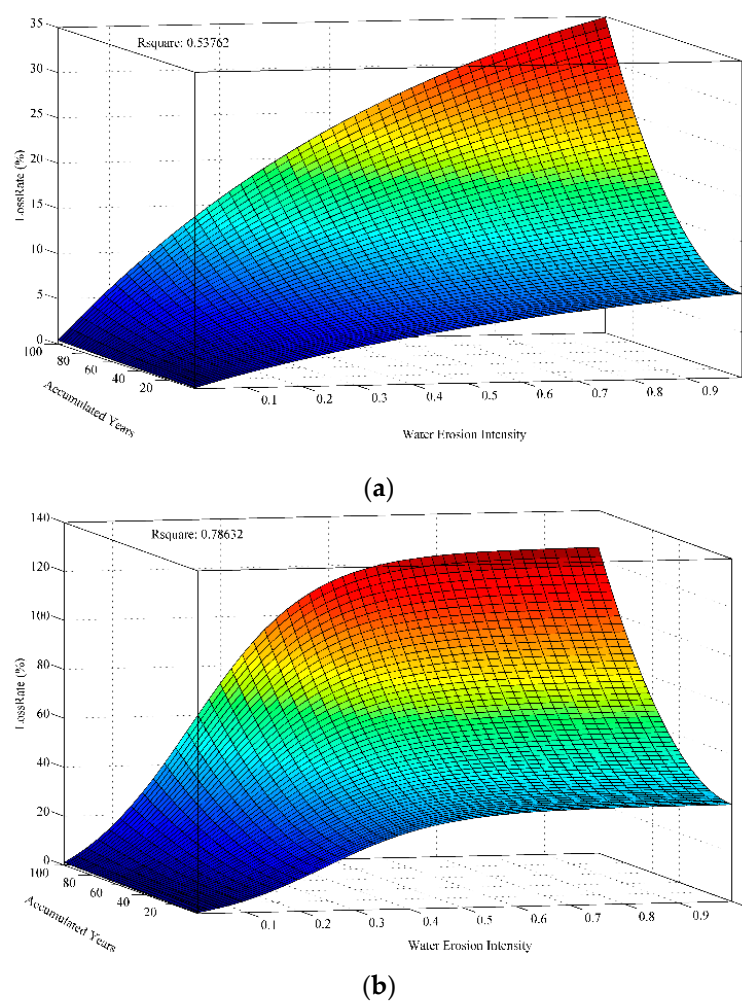


Figure 4. Cumulative loss surface for long-term accumulated water erosion in the Huaihe River basin (a) 4342980; (b) 4342840.

The 3D surfaces “water erosion intensity-cumulative years-loss rate” fit well. The R-square is 0.54 in Figure 4a and 0.78 in Figure 4b, both of which reflect a strong relationship between accumulated water and soil loss, tillage years and crop yield loss. Figure 4a shows that the maximum potential loss rate for one year is 9%. The maximum potential loss rate for 100 years is 35%. Figure 4b shows that the maximum potential loss rate for one year is 40%, and the maximum potential loss rate for 100 years

is 100%. Both figures indicate that long-term water and soil loss have an accumulated effect on crop yield loss. Losses in crop yield increase with increasing tillage years, and the loss is irreversible.

The minimum loss for one year is almost zero, and the minimum accumulated productivity loss is 0.2%, indicating that farmland productivity can be significantly maintained with soil and water conservation measures. Inappropriate tillage practices may make the region’s productivity loss rise to 100% in the future 100 years. However, the loss can be reduced with proper soil and water conservation measures, making the case for the importance of soil and water conservation practices on agricultural productivity.

3.4. Spatial Differences in Long-Term Water Erosion Impacts on Productivity

In order to understand the spatial differences in long-term loss, the 3D surfaces “water erosion intensity-cumulative years-loss rate” were obtained for all of the watersheds in the study area. The basins located in the study area are as shown in Figure 5.

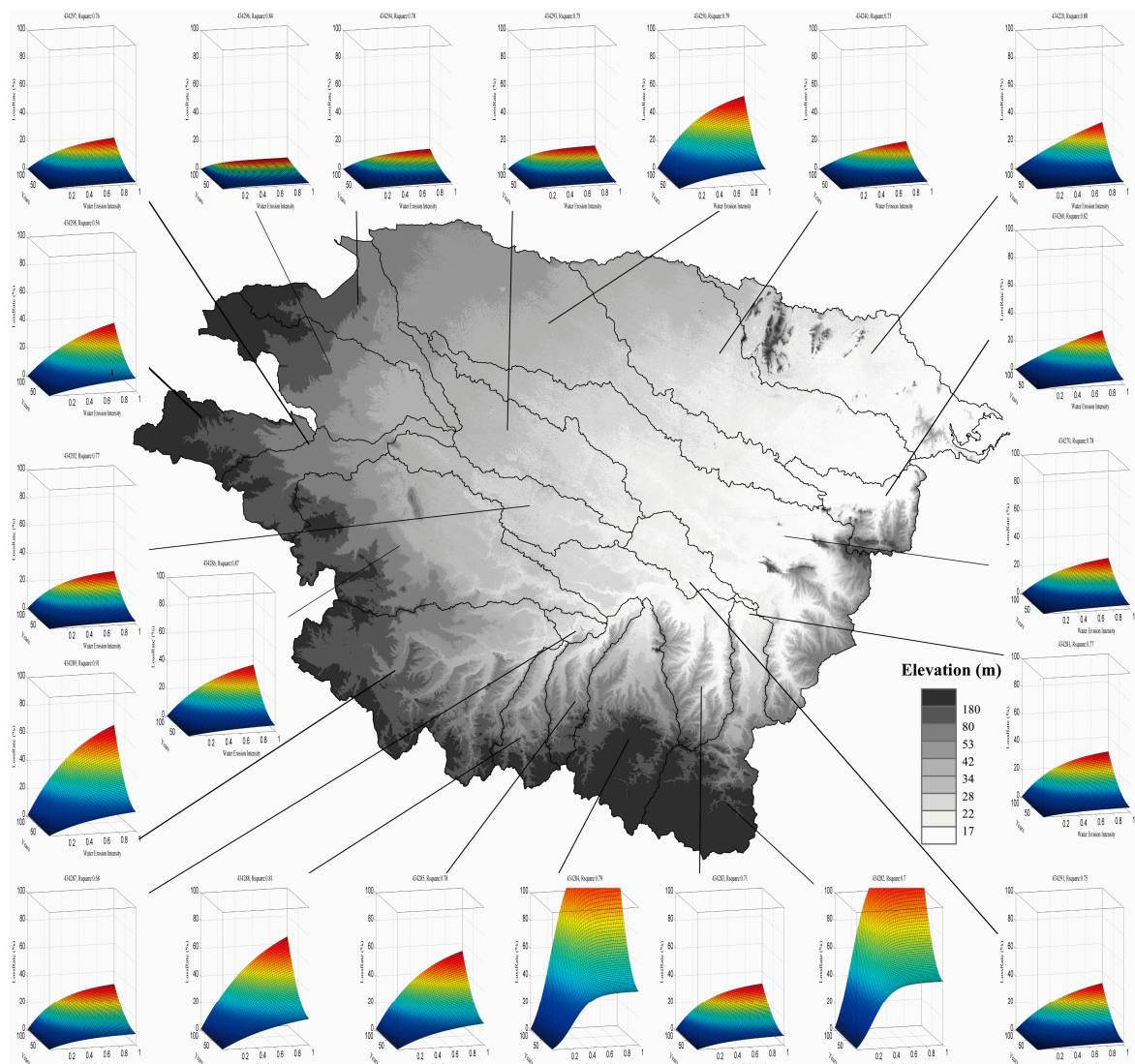


Figure 5. Spatial differences in the long-term accumulated loss for all basins in the study area.

Figure 5 shows a pattern difference in potential productivity losses for all basins located in the study area. The southern portion of the study area exhibits higher loss, especially Basins 434284 and 434282, where the largest potential productivity loss rate can reach 100%. The northern portion of the

study area, which is relatively more suitable for crops, exhibits less loss. This indicates that long-term water and soil loss have a significant impact on productivity loss, particularly in the southern region of the study area. The cumulative loss 3D surface can in this way reflect the differences in potential productivity loss.

4. Discussion

4.1. Significance of Cumulative Loss 3D Surface

Long-term water erosion has resulted in reduced farmland productivity and the reduction or even disappearance of fertile land, affecting the sustainable development of agriculture. The relationship between long-term water erosion and productivity under different soil conservation measure scenarios can more explicitly guide farming at a macroscopic scale, increasing the importance of soil and water conservation measures.

Using the accumulated loss 3D surface, we can assess the potential loss of productivity under long-term water erosion, the maximum loss of productivity and the time when the maximum loss happens. For a watershed that would reach a 100% loss rate within 100 years, planning structures should be converted to grass or forest. The earlier the 100% loss occurs, the more vulnerable the watershed productivity becomes due to soil erosion and the more urgent are reforestation measures. For a watershed that would not reach 100% loss within 100 years, the lower the loss proportion is, the more suitable the watershed becomes for planting. Higher loss proportions mean that greater investment in soil and water conservation measures is needed to improve soil and water conservation capacity. Using the accumulated loss 3D surface can effectively predict the future productivity due to long-term water erosion, quantitatively assess regional vulnerability and guide regional investment in conservation projects.

Inappropriate conservation measures have the potential of resulting in 100% productivity losses in the mountainous areas of the southern study area over the next 100 years, and this will eventually lead to desertification. This is consistent with the studies of areas in the Mediterranean at the same latitude [63]. de la Rosa et al. [63] used an ImpelERO model to study soil vulnerability caused by soil erosion in Western Europe. They found that, the maximum impact according to the long-term productivity reduction (97%) was shown for the Odiaxere-Albufeira site in the Mediterranean region and for the 2100 time horizon [63]. According to the EEA [64], the EU Mediterranean countries have severe soil erosion problems, which can reach the highest levels and lead to desertification. However, this loss can be reduced by soil and water conservation measures.

4.2. The Validation and Uncertainty of the Cumulative Loss 3D Surface

In order to verify the cumulative loss, we used long-term field experiment data from the published literature. However, some studies did not report on cumulative loss. Zhou et al. [65] conducted a field experiment in 2005–2013 in Heilongjiang. Comparing erosion conditions at an erosion of 20 cm with 30 cm, the yield loss at 30 cm of soil erosion was for the most part greater than what it was at 20 cm of soil erosion. This suggests that the more the erosion, the greater the yield loss. Reductions in maize yield in the first five study years were significant. However, after the first five years, reductions became less consistent; and in this case, no cumulative erosion was found, and yield losses did not increase. Gao et al. [23] studied the relationship between soil erosion and time in black soil and found that with the accumulation of time, erosion continues to accumulate. The experiments of Zhou et al. [65] did not set the cumulative erosion scenarios and resulted in loss without accumulation. For promotion, this study considered the erosion in the second year based on the first year's erosion, which conformed to the real situation better.

Some research has suggested that soil management contributes to reducing the soil losses and maintaining productivity, such as reduced tillage, mulching, appropriate cover crops or organic amendments [66–71]. Some research [22,23] has suggested that with a lengthened cultivation period,

productivity would be reduced and erosion would increase, meaning that there is a cumulative effect on productivity. In a study of Cambisol soil, Tenberg et al. [22] found a relationship between yield and the long-term erosion, as shown in Figure 6a. In this study, we compared our results by using the lowest level soil and water conservation measure scenarios to assess the relationship between time and yield, as shown in Figure 6b.

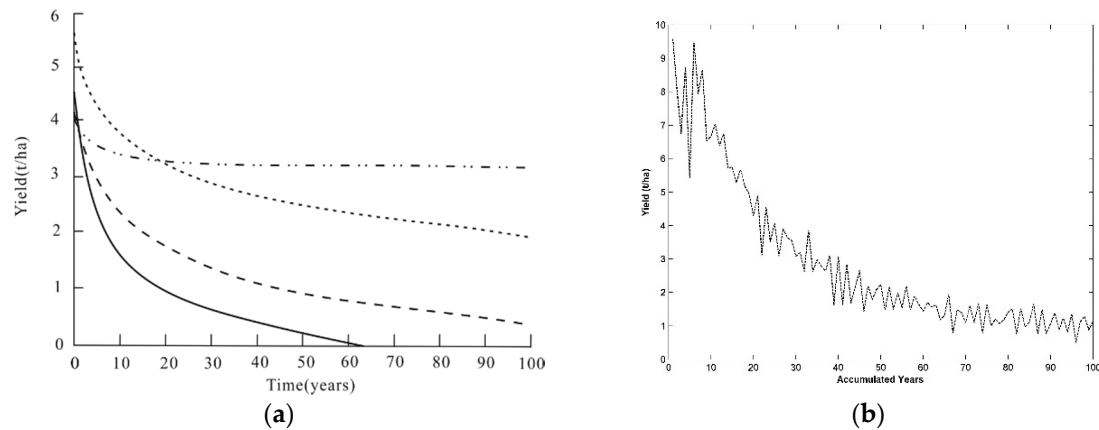


Figure 6. Yield-time relationships for (a) the Cambisol of Itapiranga [22] (—bare soil; —18% Sombrite; ····30% Sombrite; -·-·- fallow). Percentage of Sombrite refers to the rating of greenhouse shade netting; 18% gives approximate effective cover of 30%; 30% a cover of >90%; (b) the Cambisol at the 434298 watershed (— worst soil and water conservation measure scenarios).

For the same soil, different water conservation measure scenarios lead to different levels of soil erosion intensity. The worst soil and water conservation measure scenario is similar to 18% Sombrite, which means an effective vegetable coverage of 30%. The loss of yield in the Cambisol at Itapiranga [22] is found to be similar to that in Watershed 434298 in the study area, both experiencing a significant loss in productivity due to long-term water erosion. Meanwhile, the similar soil and water conservation measures would result in similar losses of productivity.

5. Conclusions

Long-term water erosion results in reduced farmland productivity and the reduction or even disappearance of fertile land, affecting the sustainable development of agriculture. The relationship between the soil erosion and productivity under different soil conservation measure scenarios can be made more explicit to guide farming on a macroscopic scale. This paper used an erosion variable-controlled method to obtain soil and water conservation measure scenarios to study the relationship between soil erosion, loss of productivity and cumulative years. It was concluded that fitting by the 3D surface can significantly and more accurately reflect the impact on productivity due to long-term water erosion than fitting by a curve. What is more, the accumulative loss 3D surface can reflect regional differences in potential productivity loss. The research can help with understanding the effects of long-term erosion on productivity.

This article seeks to add to the current body of knowledge on the impact of long-term soil erosion on productivity through a vulnerability assessment. The methodology is limited by the local parameter for the APEX model on large scales, so further research can focus on parameter adjustment. Additional research could focus on the maximum productivity loss caused by water erosion for different conservation measure projects. Research could also focus on the point when the maximum loss would occur under a current soil and water conservation measure scenario.

Acknowledgments: This study was supported by the Fund for Creative Research Groups of National Natural Science Foundation of China (No. 41321001) and also supported by the National Basic Research Program of China (973 Project): Relationship between Global Change and Environmental Risks and its Adaptation Paradigm (No. 2012CB955403), and National Key Research and Development Program (No. 2016YFA0602402). This paper was improved by comments from Jack Williams and A-Xing Zhu from the University of Wisconsin-Madison. The valuable comments and suggestions from the editor and anonymous reviewers are also greatly appreciated.

Author Contributions: Degen Lin conceived of the entire paper, analyzed the data and designed the experiments. Hao Guo and Fang Lian designed and performed the experiments, as well as analyzed the data. Fang Lian polished the text of the paper. Yaojie Yue provided technical support. Jing'ai Wang polished the text and provided project support.

Conflicts of Interest: The authors declare no conflict of interest.

References

1. Brevik, E.; Cerdà, A.; Mataix-Solera, J.; Pereg, L.; Quinton, J.; Six, J.; Van Oost, K. The interdisciplinary nature of SOIL. *Soil* **2015**, *1*, 117. [[CrossRef](#)]
2. Decock, C.; Lee, J.; Necpalova, M.; Pereira, E.; Tendall, D.; Six, J. Mitigating N₂O emissions from soil: From patching leaks to transformative action. *Soil* **2015**, *1*, 687–694. [[CrossRef](#)]
3. Smith, P.; Cotrufo, M.; Rumpel, C.; Paustian, K.; Kuikman, P.; Elliott, J.; McDowell, R.; Griffiths, R.; Asakawa, S.; Bustamante, M. Biogeochemical cycles and biodiversity as key drivers of ecosystem services provided by soils. *Soil Discuss.* **2015**, *2*, 537–586. [[CrossRef](#)]
4. Keesstra, S.D.; Quinton, J.N.; van der Putten, W.H.; Bardgett, R.D.; Fresco, L.O. The significance of soils and soil science towards realization of the United Nations Sustainable Development Goals. *Soil* **2016**, *2*, 111. [[CrossRef](#)]
5. Gang, C.; Zhou, W.; Wang, Z.; Chen, Y.; Li, J.; Chen, J.; Qi, J.; Odeh, I.; Groisman, P.Y. Comparative Assessment of Grassland NPP Dynamics in Response to Climate Change in China, North America, Europe and Australia from 1981 to 2010. *J. Agron. Crop Sci.* **2015**, *201*, 57–68. [[CrossRef](#)]
6. Gessesse, B.; Bewket, W.; Bräuning, A. Model-based characterization and monitoring of runoff and soil erosion in response to land use/land cover changes in the Modjo watershed, Ethiopia. *Land Degrad. Dev.* **2015**, *26*, 711–724. [[CrossRef](#)]
7. Keesstra, S.; Maroulis, J.; Argaman, E.; Voogt, A.; Wittenberg, L. Effects of controlled fire on hydrology and erosion under simulated rainfall. *Cuad. Investig. Geogr.* **2014**, *40*, 269–293. [[CrossRef](#)]
8. Lasanta, T.; Cerdà, A. Long-term erosional responses after fire in the Central Spanish Pyrenees: 2. Solute release. *Catena* **2005**, *60*, 81–100. [[CrossRef](#)]
9. Borrelli, P.; Märker, M.; Schütt, B. Modelling Post-Tree-Harvesting Soil Erosion and Sediment Deposition Potential in the Turano River Basin (Italian Central Apennine). *Land Degrad. Dev.* **2015**, *26*, 356–366. [[CrossRef](#)]
10. Ochoa-Cueva, P.; Fries, A.; Montesinos, P.; Rodríguez-Díaz, J.A.; Boll, J. Spatial Estimation of Soil Erosion Risk by Land-cover Change in the Andes OF Southern Ecuador. *Land Degrad. Dev.* **2015**, *26*, 565–573. [[CrossRef](#)]
11. Cao, L.; Zhang, K.; Dai, H.; Liang, Y. Modeling interrill erosion on unpaved roads in the loess plateau of China. *Land Degrad. Dev.* **2015**, *26*, 825–832. [[CrossRef](#)]
12. Department for Environment, Food and Rural Affairs. *Safeguarding Our Soils: A Strategy for England*; Department for Environment, Food and Rural Affairs: London, UK, 2009; p. 48.
13. Kraaijvanger, R.; Veldkamp, T. Grain productivity, fertilizer response and nutrient balance of farming systems in Tigray, Ethiopia: A multi-perspective view in relation to soil fertility degradation. *Land Degrad. Dev.* **2015**, *26*, 701–710. [[CrossRef](#)]
14. Erol, A.; Koşkan, Ö.; Başaran, M. Socioeconomic modifications of the universal soil loss equation. *Solid Earth* **2015**, *6*, 1025–1035. [[CrossRef](#)]
15. Musinguzi, P.; Ebanyat, P.; Tenywa, J.; Basamba, T.; Tenywa, M.; Mubiru, D. Precision of farmer-based fertility ratings and soil organic carbon for crop production on a Ferralsol. *Solid Earth* **2015**, *6*, 1063–1073. [[CrossRef](#)]

16. Wu, S.H.; Zhou, S.L.; Chen, D.X.; Wei, Z.Q.; Dai, L.; Li, X.G. Determining the contributions of urbanisation and climate change to NPP variations over the last decade in the Yangtze River Delta, China. *Sci. Total Environ.* **2014**, *472*, 397–406. [[CrossRef](#)] [[PubMed](#)]
17. Cao, X.M.; Chen, X.; Bao, A.M.; Luo, Y. Net Primary Productivity (NPP) of Oasis Changes in Trends in Xinjiang and Responses to Climate Change Analysis in 1981–2000. *Adv. Intell. Soft Comput.* **2011**, *111*, 417–424.
18. Krausmann, F.; Haberl, H.; Schulz, N.B.; Erb, K.-H.; Darge, E.; Gaube, V. Land-use change and socio-economic metabolism in Austria—Part I: Driving forces of land-use change: 1950–1995. *Land Use Policy* **2003**, *20*, 1–20. [[CrossRef](#)]
19. Haberl, H.; Fischer-Kowalski, M.; Krausmann, F.; Weisz, H.; Winiwarter, V. Progress towards sustainability? What the conceptual framework of material and energy flow accounting (MEFA) can offer. *Land Use Policy* **2004**, *21*, 199–213. [[CrossRef](#)]
20. Evans, I.S. The Selection of Class Intervals. *Trans. Inst. Br. Geogr.* **1977**, *2*, 98–124. [[CrossRef](#)]
21. West, P.C.; Gibbs, H.K.; Monfreda, C.; Wagner, J.; Barford, C.C.; Carpenter, S.R.; Foley, J.A. Trading carbon for food: Global comparison of carbon stocks vs. crop yields on agricultural land. *Proc. Natl. Acad. Sci. USA* **2010**, *107*, 19645–19648. [[CrossRef](#)] [[PubMed](#)]
22. Tenberg, A.; Da Veiga, M.; Dechen, S.C.F.; Stocking, M.A. Modelling the impact of erosion on soil productivity: A comparative evaluation of approaches on data from southern Brazil. *Exp. Agric.* **1998**, *34*, 55–71. [[CrossRef](#)]
23. Gao, X.F.; Xie, Y.; Liu, G.; Liu, B.Y.; Duan, X.W. Effects of soil erosion on soybean yield as estimated by simulating gradually eroded soil profiles. *Soil Tillage Res.* **2015**, *145*, 126–134. [[CrossRef](#)]
24. Larney, F.J.; Janzen, H.H.; Olson, B.M.; Olson, A.F. Erosion-productivity-soil amendment relationships for wheat over 16 years. *Soil Tillage Res.* **2009**, *103*, 73–83. [[CrossRef](#)]
25. Ray, N.; Adams, J. A GIS-based vegetation map of the world at the last glacial maximum (25,000–15,000 BP). *Internet Archaeol.* **2001**. [[CrossRef](#)]
26. Ye, L.M.; Van Ranst, E. Production scenarios and the effect of soil degradation on long-term food security in China. *Glob. Environ. Chang.* **2009**, *19*, 464–481. [[CrossRef](#)]
27. Dong, W.; Sullivan, P.; Stout, K. Comprehensive study of parameters for characterising three-dimensional surface topography: III: Parameters for characterising amplitude and some functional properties. *Wear* **1994**, *178*, 29–43. [[CrossRef](#)]
28. Yin, Y.; Zhang, X.; Lin, D.; Yu, H.; Shi, P. GEPIC-VR model: A GIS-based tool for regional crop drought risk assessment. *Agric. Water Manag.* **2014**, *144*, 107–119. [[CrossRef](#)]
29. Gao, C.; Gemmer, M.; Zeng, X.; Liu, B.; Su, B.; Wen, Y. Projected streamflow in the Huaihe River Basin (2010–2100) using artificial neural network. *Stoch. Environ. Res. Risk Assess.* **2010**, *24*, 685–697. [[CrossRef](#)]
30. Yin, L.; Wang, X.; Pan, J.; Gassman, P. Evaluation of APEX for daily runoff and sediment yield from three plots in the Middle Huaihe River Watershed, China. *Trans. ASABE* **2009**, *52*, 1833–1845. [[CrossRef](#)]
31. Mitchell, G.; Griggs, R.; Benson, V.; Williams, J. *The EPIC Model: Environmental Policy Integrated Climate*; Texas Agricultural Experiment Station: Temple, TX, USA, 1998.
32. Steglich, E.; Williams, J. *Agricultural Policy Environmental Extender Model-User's Manual Version 0806*; Blackland Research and Extension Center: Temple, TX, USA, 2013; pp. 1–228.
33. Lehner, B.; Verdin, K.; Jarvis, A. *HydroSHEDS Technical Documentation*; version 1.0; World Wildlife Fund US: Washington, DC, USA, 2006; pp. 1–27.
34. Gassman, P.W.; Williams, J.R.; Wang, X.; Saleh, A.; Osei, E.; Hauck, L.; Izaurrealde, C.; Flowers, J. *The Agricultural Policy Environmental Extender (APEX) Model: An Emerging Tool for Landscape and Watershed Environmental Analyses*; Center for Agricultural and Rural Development (CARD) Publications: Ames, IA, USA, 2009.
35. Sharpley, A.N.; Williams, J.R. *EPIC-Erosion/Productivity Impact Calculator: 1. Model Documentation*; United States Department of Agriculture: Washington, DC, USA, 1990.
36. Gassman, P.W.; Williams, J.R.; Benson, V.W.; Izaurrealde, R.C.; Hauck, L.M.; Jones, C.A.; Atwood, J.D.; Kiniry, J.R.; Flowers, J.D. Historical development and applications of the EPIC and APEX models. In Proceedings of the 2004 ASAE Annual Meeting, Ottawa, ON, Canada, 1–4 August 2004.
37. Gruen, A.; Akca, D. Least squares 3D surface and curve matching. *ISPRS J. Photogramm. Remote Sens.* **2005**, *59*, 151–174. [[CrossRef](#)]
38. IUCN. *UNEP-WCMC, the World Database on Protected Areas (WDPA)*; UNEP-WCMC: Cambridge, UK, 2015.

39. Friedl, M.A.; Sulla-Menashe, D.; Tan, B.; Schneider, A.; Ramankutty, N.; Sibley, A.; Huang, X. MODIS Collection 5 global land cover: Algorithm refinements and characterization of new datasets. *Remote Sens. Environ.* **2010**, *114*, 168–182. [[CrossRef](#)]
40. Simard, M.; Pinto, N.; Fisher, J.B.; Baccini, A. Mapping forest canopy height globally with spaceborne lidar. *J. Geophys. Res. Biogeosci.* **2011**. [[CrossRef](#)]
41. Miliareisis, G.C.; Argialas, D. Segmentation of physiographic features from the global digital elevation model/GTOPO30. *Comput. Geosci.* **1999**, *25*, 715–728. [[CrossRef](#)]
42. IIASA, FAO. *Global Agro-Ecological Zones-Model Documentation (GAEZ v. 3.0)*; International Institute of Applied Systems Analysis & Food and Agricultural Organization: Laxenburg, Austria; Rome, Italy, 2012.
43. Batjes, N. ISRIC-WISE Derived Soil Properties on a 5 by 5 Arc-Minutes Global Grid. Version 1.2. Available online: <http://www.isric.org/data/isric-wise-derived-soil-properties-5-5-arc-minutes-global-grid-version-12> (accessed on 12 July 2016).
44. Warszawski, L.; Frieler, K.; Huber, V.; Piontek, F.; Serdeczny, O.; Schewe, J. The inter-sectoral impact model intercomparison project (ISI-MIP): Project framework. *Proc. Natl. Acad. Sci. USA* **2014**, *111*, 3228–3232. [[CrossRef](#)] [[PubMed](#)]
45. Vitousek, P.M.; Mooney, H.A.; Lubchenco, J.; Melillo, J.M. Human domination of Earth's ecosystems. *Science* **1997**, *277*, 494–499. [[CrossRef](#)]
46. Sacks, W.J.; Deryng, D.; Foley, J.A.; Ramankutty, N. Crop planting dates: An analysis of global patterns. *Glob. Ecol. Biogeogr.* **2010**, *19*, 607–620. [[CrossRef](#)]
47. China Meteorological Administration. China's Crop Growth and Soil Moisture Late Value Farmland Collection Data. Available online: http://data.cma.cn/data/detail/dataCode/AGME_AB2_CHN_TEN.html (accessed on 14 June 2016).
48. Tan, G.; Shibasaki, R. Global estimation of crop productivity and the impacts of global warming by GIS and EPIC integration. *Ecol. Model.* **2003**, *168*, 357–370. [[CrossRef](#)]
49. Mueller, N.D.; Gerber, J.S.; Johnston, M.; Ray, D.K.; Ramankutty, N.; Foley, J.A. Closing yield gaps through nutrient and water management. *Nature* **2012**, *490*, 254–257. [[CrossRef](#)] [[PubMed](#)]
50. Rogelj, J.; den Elzen, M.; Höhne, N.; Fransen, T.; Fekete, H.; Winkler, H.; Schaeffer, R.; Sha, F.; Riahi, K.; Meinshausen, M. Paris Agreement climate proposals need a boost to keep warming well below 2 °C. *Nature* **2016**, *534*, 631–639. [[CrossRef](#)] [[PubMed](#)]
51. Williams, J.R.; Izaurralde, R. The APEX model. In *Watershed Models*; Vijay, P., Donald, K., Eds.; CRC Press: Boca Raton, FL, USA, 2006; pp. 437–482. Available online: https://books.google.co.jp/books?hl=zh-CN&lr=&id=mn8Foj3rAwQC&oi=fnd&pg=PA437&dq=The+APEX+model&ots=o9SMI-FN0z&sig=7D_S58VoOklykMnuNHvZ7qMsut#v=onepage&q=The%20APEX%20model&f=false (accessed on 14 June 2016).
52. Wischmeier, W.H.; Smith, D.D. Predicting Rainfall Erosion Losses—A Guide to Conservation Planning. Available online: <http://naldc.nal.usda.gov/download/CAT79706928/PDF> (accessed on 12 July 2016).
53. Onstad, C.; Foster, G. Erosion modeling on a watershed (Soil). *Trans. ASAE* **1975**, *18*, 288–292. [[CrossRef](#)]
54. Renard, K.G.; Foster, G.; Weesies, G.; McCool, D.; Yoder, D. *Predicting Soil Erosion by Water: A Guide to Conservation Planning with the Revised Universal Soil Loss Equation (RUSLE)*; United States Department of Agriculture: Washington, DC, USA, 1997; Volume 703.
55. Williams, J.R.; Izaurralde, R.C.; Steglich, E.M. *Agricultural Policy/Environmental Extender Model*; Theoretical Documentation, Version 0806; Blackland Research and Extension Center: Temple, TX, USA, 2008.
56. Stoorvogel, J.; Smaling, E.A.; Janssen, B. Calculating soil nutrient balances in Africa at different scales. *Fertil. Res.* **1993**, *35*, 227–235. [[CrossRef](#)]
57. Sparovek, G.; Schnug, E. Temporal erosion-induced soil degradation and yield loss. *Soil Sci. Soc. Am. J.* **2001**, *65*, 1479–1486. [[CrossRef](#)]
58. Lal, R. Soil erosion and the global carbon budget. *Environ. Int.* **2003**, *29*, 437–450. [[CrossRef](#)]
59. Zimmerman, D.W. Teacher's corner: A note on interpretation of the paired-samples *t* test. *J. Educ. Behav. Stat.* **1997**, *22*, 349–360. [[CrossRef](#)]
60. Lee, G.; Bae, J.W.; Oh, N.; Hong, J.H.; Moon, I.-C. Simulation experiment of disaster response organizational structures with alternative optimization techniques. *Soc. Sci. Comput. Rev.* **2014**. [[CrossRef](#)]
61. Norušis, M.J. *IBM SPSS Statistics 19 Guide to Data Analysis*; Prentice Hall: Upper Saddle River, NJ, USA, 2011.

62. Kent State University. SPSS Tutorials Paired Samples *t* Test. Available online: <http://libguides.library.kent.edu/SPSS/PairedSamplestTest> (accessed on 12 July 2016).
63. De la Rosa, D.; Moreno, J.; Mayol, F.; Bonson, T. Assessment of soil erosion vulnerability in western Europe and potential impact on crop productivity due to loss of soil depth using the ImpelERO model. *Agric. Ecosyst. Environ.* **2000**, *81*, 179–190. [[CrossRef](#)]
64. EEA. *Environment in the European Union at the Turn of the Century*; Office des Publications, European Environment Agency: Luxembourg City, Luxembourg, 1999.
65. Zhou, K.Q.; Sui, Y.Y.; Liu, X.B.; Zhang, X.Y.; Jin, J.; Wang, G.H.; Herbert, S.J. Crop rotation with nine-year continuous cattle manure addition restores farmland productivity of artificially eroded Mollisols in Northeast China. *Field Crops Res.* **2015**, *171*, 138–145. [[CrossRef](#)]
66. Novara, A.; Gristina, L.; Saladino, S.; Santoro, A.; Cerdà, A. Soil erosion assessment on tillage and alternative soil managements in a Sicilian vineyard. *Soil Tillage Res.* **2011**, *117*, 140–147. [[CrossRef](#)]
67. Cerdà, A.; González-Pelayo, Ó.; Giménez-Morera, A.; Jordán, A.; Pereira, P.; Novara, A.; Brevik, E.C.; Prosdocimi, M.; Mahmoodabadi, M.; Keesstra, S. Use of barley straw residues to avoid high erosion and runoff rates on persimmon plantations in Eastern Spain under low frequency–high magnitude simulated rainfall events. *Soil Res.* **2016**, *54*, 154–165. [[CrossRef](#)]
68. Prosdocimi, M.; Jordán, A.; Tarolli, P.; Keesstra, S.; Novara, A.; Cerdà, A. The immediate effectiveness of barley straw mulch in reducing soil erodibility and surface runoff generation in Mediterranean vineyards. *Sci. Total Environ.* **2016**, *547*, 323–330. [[CrossRef](#)] [[PubMed](#)]
69. García-Díaz, A.; Allas, R.B.; Gristina, L.; Cerdà, A.; Pereira, P.; Novara, A. Carbon input threshold for soil carbon budget optimization in eroding vineyards. *Geoderma* **2016**, *271*, 144–149. [[CrossRef](#)]
70. Yazdanpanah, N.; Mahmoodabadi, M.; Cerdà, A. The impact of organic amendments on soil hydrology, structure and microbial respiration in semiarid lands. *Geoderma* **2016**, *266*, 58–65. [[CrossRef](#)]
71. Keesstra, S.; Pereira, P.; Novara, A.; Brevik, E.C.; Azorin-Molina, C.; Parras-Alcántara, L.; Jordán, A.; Cerdà, A. Effects of soil management techniques on soil water erosion in apricot orchards. *Sci. Total Environ.* **2016**, *551*, 357–366. [[CrossRef](#)] [[PubMed](#)]



© 2016 by the authors; licensee MDPI, Basel, Switzerland. This article is an open access article distributed under the terms and conditions of the Creative Commons Attribution (CC-BY) license (<http://creativecommons.org/licenses/by/4.0/>).